THE INSTITUTE FOR SYSTEMS RESEARCH

ISR TECHNICAL REPORT 2018-01

Dynamic Dimension Reduction for Thin-Film Deposition Reaction Network Models

Raymond Adomaitis

Preprint, 11th IFAC Symposium on Dynamics and Control of Process Systems,
including Biosystems
June 6-8, 2016. NTNU, Trondheim, Norway

Dynamic dimension reduction for thin-film deposition reaction network models

Raymond A. Adomaitis *

* *Chemical & Biomolecular Engineering, Institute for Systems Research, University of Maryland, College Park, MD 20742 USA (e-mail: adomaiti@umd.edu).*

Abstract: A prototype thin-film deposition model is developed and subsequently used in a sequence of model reduction procedures, ultimately reducing the dynamic dimension from six to one with essentially no loss in accuracy to the dynamics of the deposition process. The species balance model consists of a singular perturbation problem of nonstandard form which first is numerically solved following the approach of Daoutidis (2015). An alternative strategy then is presented, consisting of a reaction factorization procedure which facilitates the solution of the outer solution of the singular perturbation problem and provides unique physical insight into the conserved quantities (reaction invariants) identified by the elimination of redundant dynamic modes. Further reduction in dynamic dimension then is achieved through a second factorization focused only on the major reaction species. This second reduction procedure identifies pseudo-equilibria of finite-rate properties and introduces an additional level of complexity to the challenges of identifying consistent initial conditions for DAE systems.

Keywords: Differential equations; model reduction; singular perturbation method; time constants; chemical industry; reaction invariants

1. INTRODUCTION

There is a rich history of research in model reduction methods for chemical reaction networks, especially for homogenous systems. Recently, Daoutidis (2015) reviewed some of the reaction network model reduction literature in the context of differential-algebraic equations (DAEs) produced by the reduction procedure. The objective of this work is to present the details of implementing a reaction-factorization approach we have developed to reduce the dynamic dimension of thin-film deposition kinetics models; we compare it to methods presented in Daoutidis (2015) using a prototype deposition reaction model. Our motivation for dynamic model reduction is not for computational efficiency, but to understand the true minimal dynamic dimension of thin-film deposition models so as to obtain a better fundamental understanding of the dynamics of these processes.

Consider the simplified gas/surface reaction network (RN) and the net-forward rates associated with each reaction step listed in Table 1 and shown in Fig. 1 where M and D are gas-phase monomer and dimer species with number concentrations $[M]$ and $[D]$ in m^{-3}. Species A is an adsorbed surface species with number concentration $[A]$ m^{-2} while B represents the element of precursor M that is incorporated into the bulk film and $\mathrm{A}^{\ddagger}$ the transition state of the final irreversible reaction. Note that any by-products of the irreversible deposition reaction are omitted from this example. Sites open to adsorption S are consumed during adsorption of M and regenerated as bulk film B is created. The concentration of B $[B]$ also has units m^{-2}; its value can grow infinitely large because $[B]$ represents the total number of atoms deposited per unit surface area.

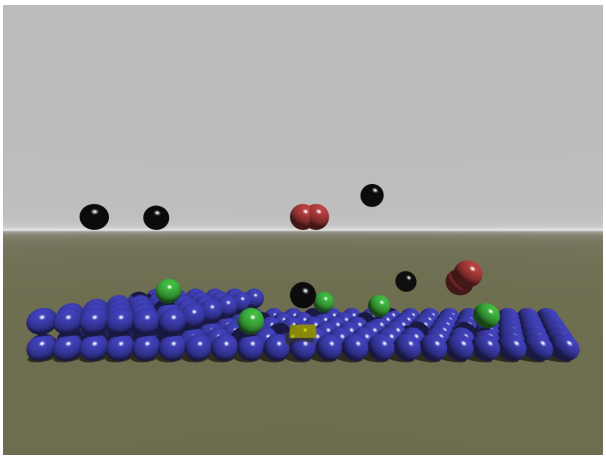

Fig. 1. A prototypical deposition system and the associated gas-phase and surface reactions. Monomer species M are shown in black, the dimer D in red, adatoms A in green, bulk film elements B in blue, and a representative adsorption site S as the yellow rectangular prism.

The first three reactions of Table 1 are reversible and the first is modeled as being barrierless in the forward direction, and so no transition state is defined for the adsorption process. The reaction between M and D is a gas phase reaction while the remainder are surface reactions.

⋆ The author gratefully acknowledges the support of the US National Science Foundation through grants CBET1160132 and CBET1438375.

For this and other heterogeneous deposition RN, we can write the number concentration material balance for each species X_j, $j = 0, \ldots, n_s - 1$ as

$$\frac{d}{dt}\phi_i[X_j] = \frac{1}{\epsilon}\sum_{k=0}^{n_g-1} Q_{j,k}g_k + \sum_{k=0}^{n_f-1} P_{j,k}f_k \tag{1}$$

for phase ϕ_i, $i = 1, \ldots, n_p - 1$ where in our two-phase system ϕ_1 represents the area of the reaction surface (in m^2) and ϕ_0 the volume (m^3) of the gas phase. Of course (1) can be rewritten in terms of the vector of molar quantities $\mathbf{m}$ for the complete set species over all of the phases

$$\frac{d\mathbf{m}}{dt} = \frac{1}{\epsilon}\mathbf{Q}\mathbf{g} + \mathbf{P}\mathbf{f} \tag{2}$$

subject to the specified initial condition

$$\mathbf{m}(0) = \mathbf{m}_o \tag{3}$$

with species molar quantities and concentrations

$$\mathbf{m} = \begin{bmatrix} D \\ A \\ M \\ A^\ddagger \\ S \\ B \end{bmatrix} \qquad \mathbf{c} = \begin{bmatrix} [D] \\ [A] \\ [M] \\ [A^\ddagger] \\ [S] \\ [B] \end{bmatrix} = \begin{bmatrix} D/\phi_0 \\ A/\phi_1 \\ M/\phi_0 \\ A^\ddagger/\phi_1 \\ S/\phi_1 \\ B/\phi_1 \end{bmatrix}. \tag{4}$$

Reaction stoichiometic coefficients are split between the two arrays

$$\mathbf{Q} = \begin{bmatrix} 1 & 0 \\ 0 & -1 \\ -2 & 0 \\ 0 & 1 \\ 0 & 0 \\ 0 & 0 \end{bmatrix}, \quad \mathbf{P} = \begin{bmatrix} 0 & 0 \\ 1 & 0 \\ -1 & 0 \\ 0 & -1 \\ -1 & 1 \\ 0 & 1 \end{bmatrix},$$

with those net forward reactions that ultimately will be treated as equilibrium relations

$$\mathbf{g} = \begin{bmatrix} g_0 \\ g_1 \end{bmatrix} = \begin{bmatrix} \phi_0(K_0[M]^2 - [D]) \\ \phi_1(K_2[A] - [A^\ddagger]) \end{bmatrix} \tag{5}$$

and the finite-rate processes

$$\mathbf{f} = \begin{bmatrix} f_0 \\ f_1 \end{bmatrix} = \begin{bmatrix} \phi_1 k_1(K_1[M][S] - [A]) \\ \phi_1 k_3[A^\ddagger] \end{bmatrix}. \tag{6}$$

The time constant ϵ has units of (s) and should be thought of as an artificial construct that makes possible writing the species balance equations (2). Finite, but small, values of ϵ correspond to the reactions (5) dynamically relaxing to chemical equilibrium defined by $\mathbf{Q}\mathbf{g} = \mathbf{0}$. It is possible to solve (2-3) directly for finite ϵ using a numerical integration technique suitable for stiff problems, although this solution can only be considered the true solution when $\epsilon \to 0$.

To give some idea of the dynamics to be expected for the case $\epsilon \to 0$, let us first consider a numerical solution to (2) for small, but finite $0 < \epsilon \ll 1$. We first set $K_0 = K_1 = 1$ m^3, $K_2 = 1$, $k_1 = k_3 = 1\ \mathrm{s}^{-1}$, $\phi_1 = 1\ \mathrm{m}^2$, $\phi_0 = 1\ \mathrm{m}^3$ (these correspond to the values used in Adomaitis (2016) except for k_2 where it was set to a value of 2 in the cited work) and choose the specified initial condition (3) to be

$$\mathbf{m}_o = [0, 0, 1, 0, 1, 0]^\intercal. \tag{7}$$

noting that $\mathbf{m}_o$ and $\mathbf{c}_o$ will have numerically identical values given our selected values of ϕ_i.

Table 1. Elementary reaction steps and net-forward reaction rates.

reaction			net forward rate		
2M	$\leftrightharpoons$	D	$(1/\epsilon)g_0$	s^{-1}	m^{-3}
S + M	$\leftrightharpoons$	A	f_0	s^{-1}	m^{-2}
A	$\leftrightharpoons$	$\mathrm{A}^\ddagger$	$(1/\epsilon)g_1$	s^{-1}	m^{-2}
$\mathrm{A}^\ddagger$	$\rightarrow$	B + S	f_1	s^{-1}	m^{-2}

Recalling the elements of $\mathbf{m}$ in (4), the specified set of initial conditions of (7) corresponds to a pure monomer gas phase and a bare growth surface. Setting $\epsilon = 0.1$ s, we observe the dynamics of the 6 ODE system in Fig. 2 (left). In the time period shortly after $t = 0$, monomer M and dimer species D relax to a pseudo-equilibrium; that brief time segment is followed by a much longer period of consumption of M (and consequently D) through the adsorption process. Likewise, at a time scale that is slower than that of the gas-phase equilibration, we observe the saturation of the growth surface with A, a period that is also followed by a slow decay to zero. These dynamics are naturally mirrored by the those of the surface sites S. Finally, the bulk species B concentration continuously increases and only asymptotically ends as all gas- and surface-phase species are consumed. Overall, we observe three distinct time scales in the dynamics displayed in Fig. 2 (left).

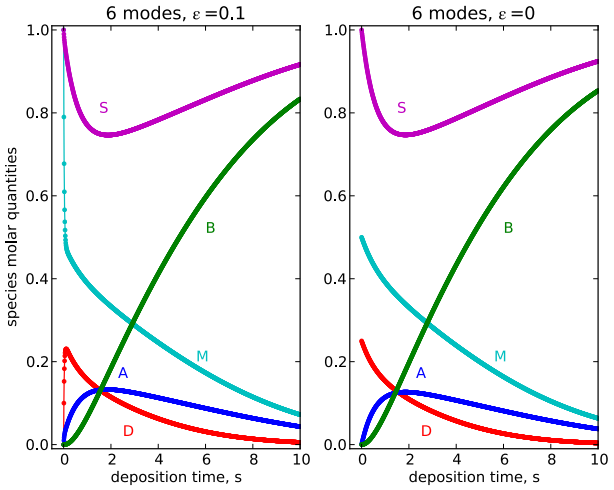

Fig. 2. Integration results for the six dynamic mode system for small finite ϵ (left) and $\epsilon \to 0$ (right).

2. SOLVING THE SINGULAR PERTURBATION PROBLEM

From Daoutidis (2015), we recognize (2) as a singularly perturbed system in nonstandard form. Because $\mathbf{Q}$ and $\partial\mathbf{g}/\partial\mathbf{m}$ are full column- and row-rank, respectively (this should be obvious by direct inspection), taking the limit $\epsilon \to 0$ will ultimately produce the pseudo-equilibrium manifold

$$\mathcal{Q} = \{\mathbf{m} : \mathbf{g} = \mathbf{0}, \mathbf{h} = \mathbf{0}\} \tag{8}$$

where the 4 additional relationships $\mathbf{h} = \mathbf{0}$ define the values of variables in $\mathbf{m}$ that are not computed using $\mathbf{g} = \mathbf{0}$. Defining the column vector γ by the elements

$$\gamma_i = \lim_{\epsilon \to 0} \frac{g_i}{\epsilon}$$

our original material balances (2) become

$$\frac{d\mathbf{m}}{dt} = \mathbf{Q}\gamma + \mathbf{Pf} \tag{9}$$

$$\mathbf{0} = \mathbf{g} \tag{10}$$

in the limit $\epsilon \to 0$. Daoutidis (2015) shows that the index of DAE system (9-10) can be reduced by computing

$$\gamma = -(\mathbf{L_Q g}(\mathbf{m}))^{-1}\mathbf{L_{Pf}}\mathbf{g}(\mathbf{m})$$

where the elements of the arrays above (with row index i and column index j) are the Lie derivatives

$$L_{\mathbf{Q}_j} g_i(\mathbf{m}) = \frac{\partial g_i}{\partial \mathbf{m}}\mathbf{Q}_j$$

where $\mathbf{Q}_j$ is the jth column of $\mathbf{Q}$. Likewise

$$L_{\mathbf{Pf}} g_i(\mathbf{m}) = \frac{\partial g_i}{\partial \mathbf{m}}\mathbf{Pf}$$

where $\mathbf{Pf}$ is the vector of finite-rate chemical processes. For our system we find

$$\frac{\partial \mathbf{g}}{\partial \mathbf{m}} = \begin{bmatrix} -1 & 0 & 2K_0M/\phi_0 & 0 & 0 & 0 \\ 0 & K_2 & 0 & -1 & 0 & 0 \end{bmatrix},$$

$$\mathbf{L_Q g} = \begin{bmatrix} -1 - 4K_0M/\phi_0 & 0 \\ 0 & -K_2 - 1 \end{bmatrix},$$

$$\mathbf{L_{Pf}}\mathbf{g} = \begin{bmatrix} -2k_1K_0M/\phi_0\,(K_1MS\phi_1/\phi_0 - A) \\ k_1K_2\,(K_1MS\phi_1/\phi_0 - A) + k_3A^\ddagger \end{bmatrix}.$$

The diagonal form of $\mathbf{L_Q g}$ makes computing its inverse trivial, therefore, γ can immediately be written as

$$\gamma = \begin{bmatrix} \dfrac{-2k_1K_0M/\phi_0\,(K_1MS\phi_1/\phi_0 - A)}{1 + 4K_0M/\phi_0} \\ \dfrac{k_1K_2\,(K_1MS\phi_1/\phi_0 - A) + k_3A^\ddagger}{K_2 + 1} \end{bmatrix}. \tag{11}$$

2.1 Consistent initial conditions, particular solutions

With γ in hand, we can compute a particular solution to (9) provided the initial conditions $\mathbf{m}^0$ are consistent with the specified initial condition $\mathbf{m}_o$ projected onto the pseudo-equilibrium manifold $\mathcal{Q}$ defined by (8). For example, if the specified initial condition (7) corresponds to 1 mole of monomer M per unit volume and zero dimer D, the monomer/dimer species material balance and (10) are both satisfied by

$$\mathbf{m}^0 = [0.25, 0, 0.5, 0, 1, 0]^\intercal. \tag{12}$$

These initial conditions are clearly visible in Fig. 2 (right) where the results of integrating (9) are shown. Comparing the numerical solution of (9) to (2) using $\epsilon = 0.1$ in the latter, we observe essentially identical results after the rapid equilibration of the dimerization reaction for finite ϵ described earlier, a result that is to be expected.

3. ELIMINATION OF REDUNDANT DYNAMIC MODES - A REACTION FACTORIZATION APPROACH

Despite being a DAE system, computational solutions to (9) still require time-integration of the full (6) ODEs. To reduce the dynamic dimension of our system, we now describe a systematic approach to developing a dynamic model of the surface reaction processes based on performing a Gauss-Jordan factorization (Chilakapati, et al., 1998; Remmers, et al., 2015) of $\mathbf{Q}$, rewritten as

$$\mathbf{Q} = \begin{bmatrix} \mathbf{Q_t} \\ \mathbf{Q_b} \end{bmatrix} \quad \text{with} \quad \mathbf{Q_t} = \begin{bmatrix} 1 & 0 \\ 0 & -1 \end{bmatrix}.$$

We note that in this example $\mathbf{Q_t} = \mathbf{Q_t}^{-1}$, which will generally not the case; in fact, in some situations where reaction expressions are incorrectly formulated, $\mathbf{Q_t}^{-1}$ may not even exist [1]. The Gauss-Jordan factorization procedure to decouple the g_i then can be carried out by

$$\begin{bmatrix} \mathbf{Q_t}^{-1} & \mathbf{0} \\ -\mathbf{Q_b}\mathbf{Q_t}^{-1} & \mathbf{I} \end{bmatrix} \frac{d\mathbf{m}}{dt} = \begin{bmatrix} \mathbf{Q_t}^{-1} & \mathbf{0} \\ -\mathbf{Q_b}\mathbf{Q_t}^{-1} & \mathbf{I} \end{bmatrix} \left(\frac{1}{\epsilon}\mathbf{Qg} + \mathbf{Pf}\right)$$

$$= \frac{1}{\epsilon}\begin{bmatrix} \mathbf{I} \\ \mathbf{0} \end{bmatrix}\mathbf{g} + \begin{bmatrix} \mathbf{Q_t}^{-1}\mathbf{P_t} \\ \mathbf{P_b} - \mathbf{Q_b}\mathbf{Q_t}^{-1}\mathbf{P_t} \end{bmatrix}\mathbf{f}.$$

It is clear that when $\mathbf{Q_t}^{-1}$ exists (and it does for this system), we obtain the DAE system

$$\begin{bmatrix} -\mathbf{Q_b}\mathbf{Q_t}^{-1} & \mathbf{I} \end{bmatrix} \frac{d\mathbf{m}}{dt} = \begin{bmatrix} \mathbf{P_b} - \mathbf{Q_b}\mathbf{Q_t}^{-1}\mathbf{P_t} \end{bmatrix}\mathbf{f} \tag{13}$$

$$\mathbf{0} = \mathbf{g} \tag{14}$$

for $\epsilon \to 0$. For our system, recalling that the species molar quantity vector $\mathbf{m}$ is defined by (4), we find that (13) becomes

$$\frac{d}{dt}\begin{bmatrix} 2D + M \\ A + A^\ddagger \\ S \\ B \end{bmatrix} = \begin{bmatrix} -1 & 0 \\ 1 & -1 \\ -1 & 1 \\ 0 & 1 \end{bmatrix}\mathbf{f} = \mathbf{Rf}. \tag{15}$$

Clearly there is redundancy in the differential equations (15) given that the column span of the array premultiplying the vector of finite-rate processes $\mathbf{f}$ has dimension 2. Therefore, we continue our factorization procedure by first defining the submatrices

$$\mathbf{R_t} = \begin{bmatrix} -1 & 0 \\ 1 & -1 \end{bmatrix} \qquad \mathbf{R_b} = \begin{bmatrix} -1 & 1 \\ 0 & 1 \end{bmatrix}$$

and so $\mathbf{R_t}^{-1}$ can be found as

$$\mathbf{R_t}^{-1} = \begin{bmatrix} -1 & 0 \\ -1 & -1 \end{bmatrix}.$$

Thus, the next step in the factorization procedure requires the computation of

$$\begin{bmatrix} \mathbf{R_t}^{-1} & \mathbf{0} \\ -\mathbf{R_b}\mathbf{R_t}^{-1} & \mathbf{I} \end{bmatrix}\begin{bmatrix} \mathbf{P_b} - \mathbf{Q_b}\mathbf{Q_t}^{-1}\mathbf{P_t} \end{bmatrix} =$$

$$\begin{bmatrix} -1 & 0 & 0 & 0 \\ -1 & -1 & 0 & 0 \\ 0 & 1 & 1 & 0 \\ 1 & 1 & 0 & 1 \end{bmatrix}\begin{bmatrix} -1 & 0 \\ 1 & -1 \\ -1 & 1 \\ 0 & 1 \end{bmatrix} = \begin{bmatrix} 1 & 0 \\ 0 & 1 \\ 0 & 0 \\ 0 & 0 \end{bmatrix}.$$

Premultiplying the left-most term of (15) by the left-most array above gives

$$d(A + A^\ddagger + S)/dt = 0 \tag{16}$$

$$d(2D + M + A + A^\ddagger + B)/dt = 0 \tag{17}$$

two new states whose physical meaning will be discussed next.

[1] A good example is the Wei-Prater isomerization example involving three isomers and three equilibrium reactions between the species: it is easy to prove that the three equilibrium reactions cannot be independently specified, leading to a noninvertible $\mathbf{Q_t}^{-1}$ in our approach.

3.1 Interpretation of the conserved modes

The results of this relatively simple operation are far-reaching. First, we observe that two conserved (instantaneous) quantities w_0 and w_1 are generated from the zeroing-out of the f_i coefficients in the bottom two rows of the expression above and are defined as

$$w_0 = A + A^\ddagger + S \tag{18}$$

$$w_1 = 2D + M + A + A^\ddagger + B. \tag{19}$$

The constant w_0 in (18) represents the maximum number of open adsorption sites on the reaction surface, and so the sum of number of adsorbed species plus the remaining number of open adsorption sites must be constant. The constant w_1 corresponds to the total number of deposition element atoms in this isolated system, where the dimer D contains two of the atoms, and all of the other species contain a single atom. Given the clear physical significance of w_0 and w_1, we conclude that *the factorization procedure can reveal essential features of the reaction chemistry*[2] .

The two- (dynamic) dimensional DAE system produced by this factorization procedure is

$$\begin{aligned} \frac{d}{dt}\begin{bmatrix} 2D+M \\ 2D+M+A+A^\ddagger \end{bmatrix} &= -\begin{bmatrix} f_0 \\ f_1 \end{bmatrix} \\ \mathbf{g} &= \mathbf{0} \\ A^\ddagger + A + S &= w_0 \\ M + 2D + B + A^\ddagger + A &= w_1 \end{aligned} \tag{20}$$

We close by noting how the linear transformation used to decouple the g_i equilibrium reactions and to factor out redundant dynamic modes is closely related to the approach used by Asbjørnsen (1972) and Rodrigues, et al. (2015) to identify variant and invariant states of chemically reacting systems.

3.2 Initial conditions, particular solutions

The introduction of the two conserved quantities w_0 and w_1 must be reconciled with the specified initial condition (7); as such, we compute

$$w_0 = w_1 = 1 \text{ m}^{-2} \tag{21}$$

which both make sense given the physical interpretation of the constants. Turning to the equilibrium relationships $\mathbf{g} = \mathbf{0}$ and returning to $\mathbf{m}^0$ given in (12), we observe that the projected initial condition (12) satisfies equilibrium relationships *and* are consistent with the conserved values in (21). Therefore, (20) is integrated forward in time subject to projected initial conditions (12) given (21) to reveal (see Fig. 3, left) precisely the same dynamics of the six-mode system shown in Fig. 2, right.

4. PSEUDO-EQUILIBRIUM OF FINITE-RATE PROCESSES

In many surface adsorption-reaction processes, the concentration of surface species (adsorbed, activated, etc.) is small relative to other species, including the surface sites S. Likewise, the rates at which surface species concentrations

[2] Because the factorization is independent of the rate expressions, the conclusions drawn regarding the conserved species will hold regardless of the actual rates.

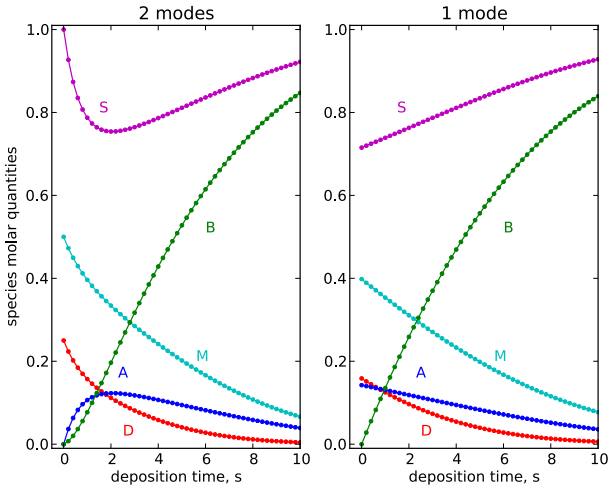

Fig. 3. Integration results for the 2-mode (left) and the 1-mode (right) systems.

change relative to the gas phase may be such that for most of the time period studied

$$\frac{d}{dt}\left(2D + M + A + A^\ddagger\right) \approx \frac{d}{dt}\left(2D + M\right) \tag{22}$$

which immediately leads to the pseudo-equilibrium relationship between the two finite-rate processes $f_0 \approx f_1$ (Adomaitis, 2016) and the question of which of the two ODEs of (20) should be retained. Writing

$$\begin{aligned} x_0 &= 2D + M \\ x_1 &= 2D + M + A + A^\ddagger, \end{aligned}$$

we observe that we cannot explicitly set a fixed initial condition $x_0(t = 0)$ because some of the gas-phase monomer will be consumed by the adsorption reaction when the specified initial conditions are projected onto the equilibrium relationships. However, we can set $x_1(t = 0)$ independently of w_0 and w_1; doing so simply then prescribes the initial value of B. Furthermore, we observe that

$$\frac{d}{dt}\left(2D + M + A + A^\ddagger\right) = -\frac{dB}{dt}$$

ultimately resulting in the one-dimensional DAE system

$$\begin{aligned} \frac{dB}{dt} &= f_1 \\ \mathbf{g} &= \mathbf{0} \\ f_0 - f_1 = p &= 0 \\ A^\ddagger + A + S &= w_0 \\ 2D + M + B + A^\ddagger + A &= w_1 \end{aligned} \tag{23}$$

where the algebraic equations of (23) define manifold $\mathcal{Q}^M$

$$\mathcal{Q}^M = \{\mathbf{m} : \mathbf{g} = \mathbf{0}, \mathbf{h} = \mathbf{0}, p = 0\}.$$

In addition to the previous algebraic constraints, projected initial conditions for (23) must also satisfy

$$k_1\left(K_1[M][S] - [A]\right) - k_3[A^\ddagger] = 0$$

which means the $\mathbf{m}^0$ of (12) no longer is valid. Projecting the specified initial conditions onto the five algebraic equations of (23) plus $B(t = 0) = 0$ gives

$$\mathbf{m}^0 = [0.158\ 0.142\ 0.398\ 0.142\ 0.716\ 0.0]. \tag{24}$$

Of course, DAE systems are well-known to present challenges to finding consistent initial conditions, particularly for high-index systems (see, e.g., Biegler (2000), Pantelides (1988)). It is interesting to see how using physically based arguments is key to finding the correct initial conditions for our deposition system after each of the sequential steps in our reduction process.

4.1 Interpretation of the reduced dynamics

Figure 3 compares the 2-mode solution (left) to the dynamics of the 1-dimensional system (right). The reduced stiffness of the 2- and 1-mode DAE systems is clearly indicated by increased step size used in the simulations. Of course, the 2-mode solution computed using our factorization procedure should be the same as the true solution to the 6-mode system for $\epsilon \to 0$, and that can be confirmed by comparing Fig. 2 (right) and Fig. 3 (left).

The projected initial conditions (24) are visible in Fig. 3 (right) and represent the instantaneous equilibration of species D, M, S, A, and $A^\ddagger$ on manifold $\mathcal{Q}^M$. The initial values of $[M]$ and $[D]$ are reduced relative to the 2-mode system's initial condition because of the consumption of the gas-phase species by the adsorption process and the production of the activated surface species $A^\ddagger$. The effect of the new pseudo-equilibrium relationship is to eliminate the initial S and A dynamics; afterwards, the dynamics of all species follows the slower dynamic phase seen in the 2- and 6-mode processes. All of the processes essentially reach the same states at $t = 10$ s, indicating that the model reduction procedure has minimal effect on the deposition process modeling accuracy.

5. AN ALTERNATIVE VIEW OF THE REDUCTION PROCESS

We summarize the model reduction process in Fig. 4 where the dynamic behavior of the finite-ϵ 6-dimensional, the 2-D, and the 1-D models are all represented by the trajectories in (M, D, A)-space produced from a common specified initial condition, together with the $\mathcal{Q}$ and $\mathcal{Q}^M$ manifolds, and the projected initial conditions.

Starting with the fictitious case of $\epsilon > 0$ (2), the trajectory representing a solution to this 6-mode model is shown as the black dotted curve in Fig. 4. It starts from specified initial condition $\mathbf{m}_o$ (3), quickly contracts to $\mathcal{Q}$, and then approaches and follows $\mathcal{Q}^M$ to the steady state $\mathbf{m}^\infty$, which represents the complete consumption of reactants in this closed system.

The particular solution of the 2-mode reduced system (20) corresponding specified initial condition $\mathbf{m}_o$ (3) is marked by the red squares of Fig. 4. For this system, the specified initial condition $\mathbf{m}_o$ is first projected onto the 2-dimensional $\mathcal{Q}$; this operation is denoted by the red line segment connecting $\mathbf{m}_o$ and the corresponding $\mathbf{m}^0$ on $\mathcal{Q}$ as the enlarged red square. As described in the discussion of Fig. 3, the primary difference between this solution and that of the case corresponding to $\epsilon > 0$ is the lack of the quick equilibration dynamics of the dimerization reaction.

Finally, we observe the trajectory corresponding to the single dynamic-mode model (23) as denoted by the yellow-filled circles of Fig. 4. Analogous to the case of the 2-mode model, the specified initial condition $\mathbf{m}_o$ is first projected onto the 1-dimensional $\mathcal{Q}^M$ (following the green line segment to the enlarged yellow circle) to which the dynamics are then constrained. Overall, the phase space is organized by the invariant structures: the 2-D $\mathcal{Q}$, 1-D $\mathcal{Q}^M$, and 0-D fixed-point $\mathbf{m}^\infty$.

6. AN OPEN REACTION SYSTEM

Let us now consider a modification to the finite-rate processes of (2) consisting of the extended stoichiometric coefficient matrix

$$\mathbf{P} = \begin{bmatrix} 0 & 0 & 1 & 0 \\ 1 & 0 & 0 & 0 \\ -1 & 0 & 0 & 1 \\ 0 & -1 & 0 & 0 \\ -1 & 1 & 0 & 0 \\ 0 & 1 & 0 & 0 \end{bmatrix},$$

and the addition of two reaction rates f_2 and f_3

$$\mathbf{f} = \begin{bmatrix} f_0 \\ f_1 \\ f_2 \\ f_3 \end{bmatrix} = \begin{bmatrix} \phi_1 k_1 (K_1[M][S] - [A]) \\ \phi_1 k_3 [A^\ddagger] \\ u_{in}[D_{in}] - u_{out}[D] \\ u_{in}[M_{in}] - u_{out}[M] \end{bmatrix} \tag{25}$$

representing the net inflow of dimer species D and monomer M, respectively. In this formulation the inlet u_{in} and outlet volumetric flow terms u_{out} have units $m^3 s^{-1}$. These changes have the effect of converting (2) from a closed (batch) system to a CSTR with a well-mixed gas phase in contact with the reaction surface.

The first step in the factorization to diagonalize the g_i proceeds exactly as before. The step that follows where redundant dynamic modes are eliminated also takes place in the same manner as before; however, it produces a different DAE system because of the addition of f_2 and f_3. What is found from the combined factorization procedure is the system:

$$\frac{d}{dt} \begin{bmatrix} 2D + M \\ 2D + M + A + A^\ddagger \\ 2D + M + A + A^\ddagger + B \end{bmatrix} = \begin{bmatrix} -f_0 + 2f_2 + f_3 \\ -f_1 + 2f_2 + f_3 \\ 2f_2 + f_3 \end{bmatrix} \tag{26}$$

$$\mathbf{g} = \mathbf{0} \tag{27}$$

$$A^\ddagger + A + S = w_0 \tag{28}$$

where we now have only one true invariant (28). Physically, this makes sense: (28) represents the conservation of surface reaction sites, a quantity unaffected by the in/outflow of species in the gas phase.

The third differential equation in (26) is invariant with respect to the true reactions of our system; is represents the total number of deposition species atoms in our system and so the dynamics of this quantity are only affected by the net inflow of the deposition species $2f_2 + f_3$. The second ODE of (26) represents the change in total number of deposition species in the gas phase and that can be reversibly desorbed from the system; the first ODE in (26) described the accumulation rate of the deposition species in the gas phase. The quasi-equilibrium manifold for (26-28) is three dimensional; it is not difficult to see that one can rewrite this system in such a way that the dynamics would be most clearly illustrated in the (D, A, B) species molar quantity space.

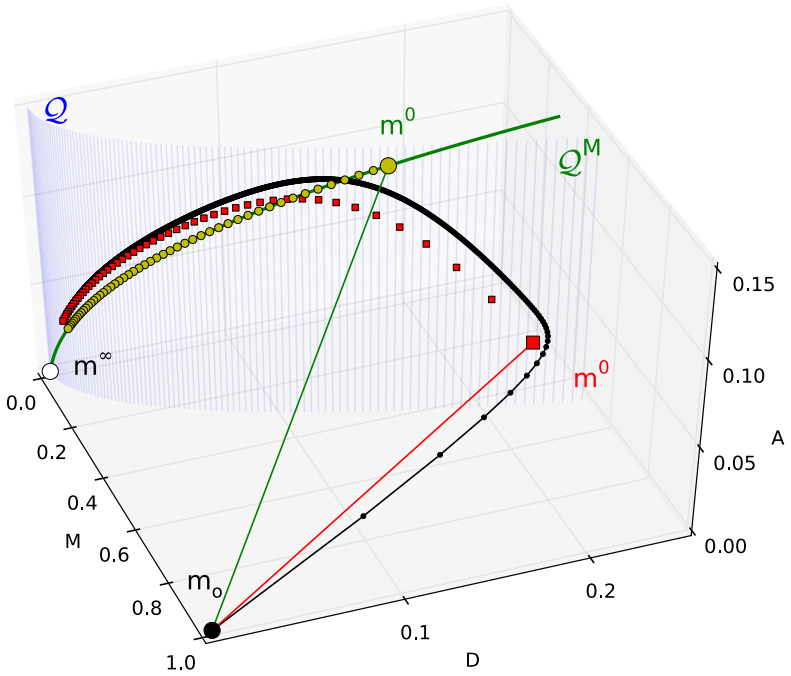

Fig. 4. Dynamics for the 6-, 2-, and 1-mode models in (M, D, A)-space showing the hierarchical relaxation to $\mathcal{Q}$ (for finite ϵ), to $\mathcal{Q}^M$, to $\mathbf{m}^\infty$.

6.1 Pseudo-equilibrium of the finite-rate processes for the open system

We note that (22) may still apply for this system and under these conditions $f_0 \approx f_1$ likewise will hold. This results in the further reduction of (26-28) to

$$\begin{aligned} \frac{d}{dt}\begin{bmatrix} 2D+M \\ B \end{bmatrix} &= \begin{bmatrix} -f_0+2f_2+f_3 \\ -f_1 \end{bmatrix} \\ \mathbf{g} &= \mathbf{0} \\ f_0 - f_1 = p &= \mathbf{0} \\ A^\ddagger + A + S &= w_0 \end{aligned} \tag{29}$$

producing a two-dimensional quasi-equilibrium manifold upon which the dynamics governed by the two ODEs of the DAE system above evolve.

6.2 Deposition rate control

In an industrial CVD reactor system, it may be desired to control the deposition rate $r = dB/dt$. For example, in a roll-to-roll large-scale reactor system, the substrate may be required to move at a uniform rate through the deposition reactor system, and control of deposition rate r is required to maintain uniform film thickness in the face of substrate temperature and other disturbances. Because direct control of the surface reaction processes generally is impossible, control can only be provided through the gas-phase inputs to the reaction system.

If the precursor is injected from a source held at a higher pressure and lower temperature relative to the reaction chamber, it may enter as an essentially pure stream of dimer D, dissociating into the equilibrium mixture according to equilibrium relationship $g_0 = 0$ under reactor chamber conditions. This means $f_2 = u - u_{out}[D]$ and $f_3 = -u_{out}[M]$ where our manipulated variable $u = u_{in}[D_{in}]$ is the molar flow of dimer D to the reactor and $u_{out} = (u - f_0)/([D] + [M])$. The consequences of our reaction factorization approach on control system design are beyond the scope of this study and will be addressed in future work; it is anticipated that the work will follow that of Asbjørnsen (1972) and Rodrigues, et al. (2015).

REFERENCES

R. A. Adomaitis, Dynamic order reduction of thin-film deposition kinetics models: A reaction factorization approach, *JVST A*, **34** 01A104 (2016).

O. A. Asbjørnsen, Reaction invariants in the control of continuous chemical reactors, *Chem. Engng Sci.*, **27** 709-717 (1972).

L. T. Biegler, *Differential-Algebraic Equations (DAEs)*, Lecture notes (2000).

A. Chilakapati, T. Ginn, and J. Szecsody, An analysis of complex reaction networks in groundwater modeling, *Water Resources Res.*, **34** 1767-1780 (1998).

P. Daoutidis, DAEs in model reduction of chemical processes: An overview, In *Surveys in Differential-Algebraic Equations II* A. Ilchmann and T. Reis, Eds., Springer, 69-102 (2015).

C. C. Pantelides, The consistent initialization of differential-algebraic systems, *SIAM J. Sci, Stat. Comput.* **9** 213-231 (1988).

E. M. Remmers, C. D. Travis, and R. A. Adomaitis, Reaction factorization for the dynamic analysis of atomic layer deposition kinetics, *Chem. Engng Sci.*, **127** 374-391 (2015).

D. Rodrigues, S. Srinivasan, J. Billeter, and D. Bonvin, Variant and invariant states for chemical reaction systems, *Comp. & Chem. Engng*, **73** 23-33 (2015).